Advances in Water Resources 74 (2014) 231–244

Contents lists available at ScienceDirect

Advances in Water Resources

journal homepage: www.elsevier.com/locate/advwatres

Intercomparison of the JULES and CABLE land surface models through assimilation of remotely sensed soil moisture in southeast Australia

Gift Dumedah *, Jeffrey P. Walker

Department of Civil Engineering, Monash University, Clayton, 3800 Victoria, Australia

ARTICLE INFO

Article history:
Received 27 March 2014
Received in revised form 24 September 2014
Accepted 26 September 2014
Available online 6 October 2014

Keywords:
Soil moisture
Model intercomparison
JULES
CABLE
Data assimilation
Evolutionary algorithms

ABSTRACT

Numerous land surface models exist for predicting water and energy fluxes in the terrestrial environment. These land surface models have different conceptualizations (i.e., process or physics based), together with structural differences in representing spatial variability, alternate empirical methods, mathematical formulations and computational approach. These inherent differences in modeling approach, and associated variations in outputs make it difficult to compare and contrast land surface models in a straight-forward manner. While model intercomparison studies have been undertaken in the past, leading to significant progress on the improvement of land surface models, additional framework towards identification of model weakness is needed. Given that land surface models are increasingly being integrated with satellite based estimates to improve their prediction skill, it is practical to undertake model intercomparison on the basis of soil moisture data assimilation. Consequently, this study compares two land surface models: the Joint UK Land Environment Simulator (JULES) and the Community Atmosphere Biosphere Land Exchange (CABLE) for soil moisture estimation and associated assessment of model uncertainty. A retrieved soil moisture data set from the Soil Moisture and Ocean Salinity (SMOS) mission was assimilated into both models, with their updated estimates validated against in-situ soil moisture in the Yanco area, Australia. The findings show that the updated estimates from both models generally provided a more accurate estimate of soil moisture than the open loop estimate based on calibration alone. Moreover, the JULES output was found to provide a slightly better estimate of soil moisture than the CABLE output at both near-surface and deeper soil layers. An assessment of the updated membership in decision space also showed that the JULES model had a relatively stable, less sensitive, and more highly convergent internal dynamics than the CABLE model.

1. Introduction

Land surface models play a crucial role in the estimation and monitoring of terrestrial state variables such as soil moisture. Land surface models use physiographic properties of the landscape, together with meteorological forcing data to simulate the water and energy fluxes between a vertical profile of soil, vegetation, and the atmosphere [2,31,47]. The monitoring of land surface soil moisture can be undertaken in three major ways: (i) through in-situ soil moisture observations, (ii) by remotely sensed observations from satellites and aircraft, and (iii) through land surface modeling. Among these three methods of acquiring soil moisture, only land surface models have the capability to evolve soil moisture forward in time – an essential requirement for planning and management purposes.

The forward estimations from land surface models are usually updated in time with satellite observations of soil moisture [7,18,36,46], through data assimilation (DA) procedures. Primarily, the DA approach improves upon the simulated output from the land surface model by updating the model state trajectories through time. This means that improved soil moisture estimates from land surface models will ultimately lead to efficient planning outcomes. Improved land surface estimates can be achieved by continued refinement of models [23,24], through changes in their structure, and direct learning from observations to enhance their reliability. An important step towards refining land surface model physics, leading to more accurate state estimates and identification of weaknesses in the model is to compare and contrast their performance against in-situ soil moisture.

Consequently, this study compares the soil moisture estimation skill of two land surface models: (i) the Joint UK Land Environment Simulator (JULES) [2], and (ii) the Community Atmosphere Biosphere Land Exchange (CABLE) model [31,47], and assesses their

* Corresponding author.
E-mail address: dgiftman@hotmail.com (G. Dumedah).

http://dx.doi.org/10.1016/j.advwatres.2014.09.011
0309-1708/

uncertainty. This study assimilates retrieved soil moisture from the Soil Moisture and Ocean Salinity (SMOS) satellite into the JULES and CABLE models, for estimation of soil moisture in the Yanco area located in southeast Australia. The Yanco area is monitored by an extensive in-situ data set (OzNet data – www.oznet.org.au) from [44], which enables subsequent validation of the updated soil moisture from both models.

Currently, the Australian Bureau of Meteorology uses the JULES model to estimate the land surface state components for its numerical weather prediction model, the Australian Community Climate and Earth-System Simulator (ACCESS). However, there is growing interest to replace the JULES model with CABLE in the near future. The CABLE model is providing the land surface component for the ACCESS version 1.3 in a test phase. An assessment of the estimated soil moisture from these models, validated with in-situ soil moisture, will provide crucial information for implementation purposes including the possibility of identifying limitations in the model structure.

This paper undertakes soil moisture assimilation into both models using the evolutionary data assimilation (EDA) procedure [17,21]. The EDA is a synthesis between the stochastic and adaptive capabilities of a computational evolutionary strategy, and the concept of temporal state updating into a unified DA procedure. The EDA has been compared against advanced DA methods such as the ensemble Kalman filter and particle filter [19,21], to illustrate its unique contributions on merging simulated model outputs with observations. As will be illustrated in the results section, an evaluation of updated members obtained from the EDA approach has the capability to quantify uncertainties for model parameters, states, input forcing data, and the spatial variation of the landscape.

It is noted that, land surface model intercomparison has been undertaken in numerous studies in the past, including [3,13,15,22,26,28,32,34,40,43]. The Project for the Intercomparison of Land-Surface Parameterization Schemes (PILPS) [25–27,40] assessed over 30 land surface models, leading to considerable improvements and better understanding of land surface models. The models in PILPS were generally evaluated in off-line experiments (i.e., driven by prescribed meteorological forcing data), with subsequent simulated outputs compared against observed fluxes. The Global Soil Wetness Project (GSWP) 1 and 2 [13–15] assessed 13 land surface models, through the examination of model sensitivity, the impact of model parameter and forcing variable uncertainty on simulated fluxes, and the provision of global land surface fluxes. The AMMA Land Surface Model Intercomparison Project (ALMIP) [3] employed about 11 land surface models, together with field campaign data, to better understand the connections between terrestrial processes and the West African monsoon. Additionally, [32] examined the sensitivity of 12 of the PILPS models, assessing the response of four model outputs (evapotranspiration, runoff, sensible heat flux, and soil moisture) to changes in five model parameters (maximum soil moisture content, effective available water content, Clapp–Hornberger b parameter [6], leaf area index, and minimum stomatal resistance). At annual scale, they found that the models have different sensitivities under different hydroclimatic conditions, and that model parameter interactions were inconsistent, with some models having high response to changes in a single model parameter.

While significant progress has been made in land surface intercomparison studies, few studies including [22] have actually intercompared several models whereby, the land surface model estimates have been updated with retrieved satellite soil moisture, and the updated estimates validated against in-situ soil moisture. It is acknowledged that other soil moisture assimilation studies have been undertaken including [1,8,12,16,35], but these studies have not intercompared multiple land surface models. This study evaluates two widely applied land surface models (JULES and CABLE), investigating their temporal changes in decision space comprising model parameters, states, and forcing data uncertainties. Moreover, the high density nature of the in-situ soil moisture stations within the study site is important, providing comprehensive space–time coverage to validate the updated soil moisture estimates at both near-surface and deeper soil layers.

2. Materials and methods

2.1. Study area, data sets, and the land surface models

This model intercomparison study was undertaken in the Yanco area located in the western plains of New South Wales, Australia with an area coverage of about 7056-km^2. The land cover in the Yanco area (shown in Fig. 1) is mainly grassland, with sparse pasture and irrigated crops. The topography is fairly flat with scattered domes, lunettes, swampy depressions, and discontinuous low river ridges associated with prior stream systems [37]. The soil is mainly loam textured, together with traces of sand and clay textured loams.

The Yanco area is highly instrumented, having a combination of Campbell water content reflectometers CS615 and CS616, and T-107 thermistors, for monitoring soil moisture and temperature conditions. The area comprises 13 monitoring stations with half-hourly soil moisture observations made at four soil layer thicknesses: 0–8 cm, 0–30 cm, 30–60 cm, and 60–90 cm. The Yanco soil moisture network is a subset of the OzNet monitoring system [44], which has been in operation since 2001.

The JULES is a tiled model with sub-grid heterogeneity for simulating the water and energy fluxes for nine surface types including: broadleaf, needleleaf, C3 (temperate) grass, C4 (tropical) grass, shrubs, urban, inland water, bare soil, and land-ice [2]. The energy budget in JULES accounts for the following components: (i) surface energy, mainly fluxes of sensible heat and moisture, and latent heat of vaporization for snow-free tiles or sublimation for snow-covered tiles, together with ground heat flux which combines radiative fluxes below vegetation canopies and conductive fluxes for the non-vegetation fraction as a function of the thickness and temperature of the surface soil layer; (ii) conductances for sensible and latent heat fluxes between the land surface and the atmosphere; (iii) canopy heat capacity; and (iv) surface evaporation drawn from saturated surfaces (e.g., lakes), soil, canopy and snow moisture stores.

The hydrology is determined for each tile by partitioning precipitation, which is distributed exponentially across the area, into interception, throughfall, runoff and infiltration. The soil hydrology, accounting for the movement of water between soil layers is based on a finite difference approximation to the Richards' equation [42]. The soil moisture extraction by vegetation is determined by root density, which is assumed to follow an exponential distribution with depth [2]. JULES represents vegetation cover through leaf area index (LAI), which is represented by maximum and minimum values for each of the 5 plant functional types, together with a 'full leaf' LAI. The LAI accounts for the available energy partitioning between soil and vegetation surfaces, and facilitates the estimation of water use by vegetation. The JULES's meteorological forcing variables and prognostic variables essential to this study are presented in Table 1.

The CABLE model is also tiled with sub-grid heterogeneity, comprising five main modules: (i) radiation, (ii) canopy micrometeorology, (iii) surface flux, (iv) soil, and (v) ecosystem carbon. The radiation accounts for the transfer and absorption of radiation by the sunlit and shaded leaves [47]. The canopy micrometeorology encompasses the surface roughness length, zero-plane

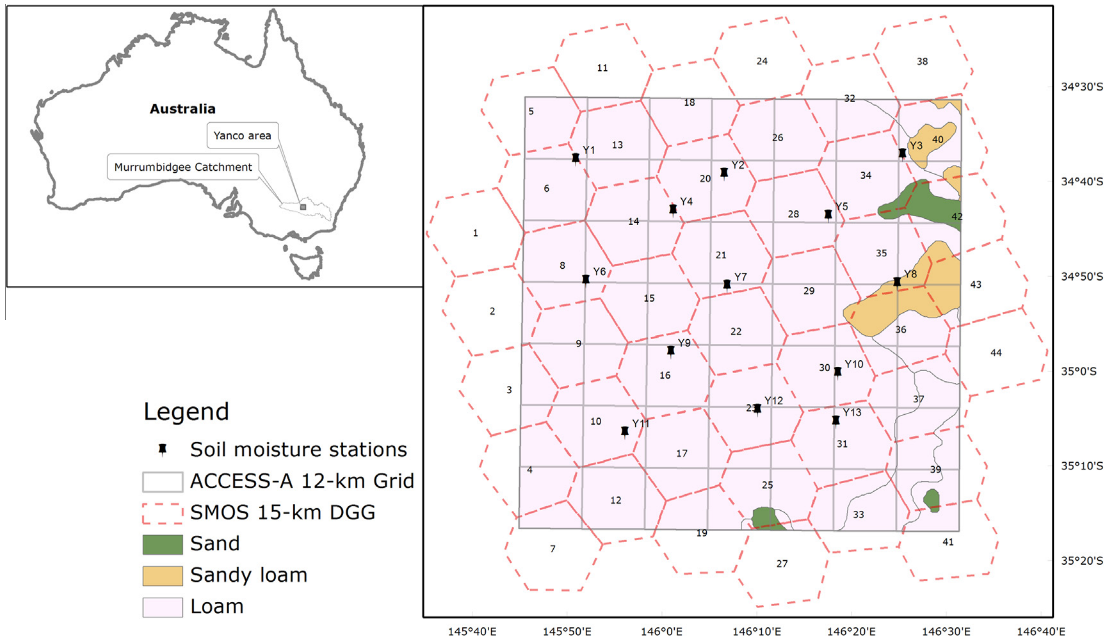

Fig. 1. The Yanco area in south-east Australia, showing the soil texture, the 15-km SMOS Disrete Global Grid (DGG), the 12-km model grid from ACCESS-A, and the in-situ OzNet soil moisture monitoring stations.

Table 1
Description of selected model parameters, states and input forcing variables for the JULES model. These model parameter intervals were estimated in concert with land cover, soil properties and meteorological forcing data in the Yanco area.

Parameter	Description	Interval
Model parameters		
b	Exponent in soil hydraulic characteristics curve	±10%
sathh	Absolute value of the soil matric suction at saturation (m)	±10%
hsatcon	Hydraulic conductivity at saturation ($kg\ m^{-2}\ s^{-1}$)	±10%
sm-sat	Soil moisture content at saturation (m^3 water per m^3 soil)	±10%
sm-crit	Soil moisture content at critical point (m^3 water per m^3 soil)	±10%
sm-wilt	Soil moisture content at wilting point (m^3 water per m^3 soil)	±10%
hcap	Dry heat capacity ($J\ m^{-3}\ K^{-1}$)	±10%
hcon	Dry thermal conductivity ($W\ m^{-1}\ K^{-1}$)	±10%
albsoil	Soil albedo	±10%
Meteorological forcing variables		
SWR	Downward shortwave radiation at the surface (W/m^2)	±10%
LWR	Downward longwave radiation at the surface (W/m^2)	±10%
rain	Rainfall ($kg\ m^{-2}\ s^{-1}$)	±10%
snow	Snowfall ($kg\ m^{-2}\ s^{-1}$)	±10%
tempr	Atmospheric temperature (K)	±10%
wind	Wind speed ($m\ s^{-1}$)	±10%
press	Surface pressure (Pa)	±10%
spHum	Atmospheric specific humidity ($kg\ kg^{-1}$)	±10%
Model state variables		
canopy	Amount of intercepted water that is held on each tile ($kg\ m^{-2}$)	Updated
tstar-t	Surface or skin temperature of each tile (K)	Updated
t-soil	Temperature of each soil layer (K)	Updated
sthuf	Soil wetness for each soil layer; mass of soil water expressed as a fraction of water content at saturation	Updated

displacement height, and aerodynamic conductance from the reference height to the air within canopy or to the soil surface. The surface flux includes the surface energy budget, transpiration, stomatal conductance, and photosynthesis of sunlit and shaded leaves. The soil module accounts for the water and energy fluxes at the soil surface and within the soil layers, whereas the ecosystem carbon component includes estimates for the respiration of stem, root and soil organic carbon decomposition [47]. The main surface types used in CABLE include: evergreen needleleaf and broadleaf, deciduous needleleaf and broadleaf, shrub, temperate and tropical grass, Tundra, crop, wetland, bare ground, lake, and ice. The soil layers in CABLE are fixed to six soil thicknesses: 2.2-cm, 5.8-cm, 15.4-cm, 40.9-cm, 108.5-cm and 287.2-cm, respectively from top to bottom, with the movement of water between layers estimated using the Richards equation [31,47]. CABLE uses the Penman–Monteith calculation to estimate evaporation from bare soils, which in turn is weighted by soil moisture in the top soil layer [31,47]. The meteorological forcing variables and prognostic variables essential for soil moisture estimation in CABLE are presented in Table 2.

The input landscape properties data including soil and land cover data sets are similar for both the JULES and CABLE models. The soil properties data set was obtained from the Digital Atlas of Australian Soils [37], comprising information on soil texture classes, along with proportion of clay content, bulk density, and saturated hydraulic conductivity [37,38]. The LAI data set was obtained from the MYD15A2 Moderate Resolution Imaging Spectroradiometer (MODIS) data at 8-day time scale and 1-km spatial resolution. The land cover information was obtained from the Australian National Dynamic Land Cover Data set [33], which was derived from the 250-m bands of MODIS.

The meteorological forcing data was obtained from the Australian Community Climate Earth-System Simulator – Australia (ACCESS-A) at hourly time scale with about ~12-km spatial resolution [4]. The ACCESS-A precipitation data was bias corrected using the daily 5-km gridded raingauge precipitation data, obtained from the Australian Water Availability Project (AWAP) through the Bureau of Meteorology [29,30]. The precipitation bias correction is conducted by matching the mean precipitation from the ACCESS-A to the average AWAP precipitation. The soil, LAI, and land cover data are mapped onto the 12-km ACCESS-A grids through a spatial overlap, and subsequent estimation of the percent coverage

Table 2
Description of selected model parameters, states and input forcing variables for the CABLE model. These model parameter intervals were estimated in concert with land cover, soil properties and meteorological forcing data in the Yanco area.

Parameter	Description	Interval
Model parameters		
clay	Fraction of soil which is clay (–)	±10%
sand	Fraction of soil which is sand (–)	±10%
silt	Fraction of soil which is silt (–)	±10%
froot	Fraction of roots in each soil layer (–)	±10%
albsoil	Snow free shortwave soil reflectance fraction (–)	±10%
bch	Parameter b, Campbell eqn 1985 (–)	±10%
css	Heat capacity of soil minerals (J/kg/C)	±10%
hyds	Hydraulic conductivity at saturation (m/s)	±10%
rhosoil	Density of soil minerals (kg/m^3)	±10%
sucs	Suction at saturation (m)	±10%
sfc	Fraction of soil volume which is water at field capacity (–)	±10%
ssat	Fraction of soil volume which is water at saturation (–)	±10%
swilt	Fraction of soil volume which is water at wilting point (–)	±10%
LAI	Leaf area index (m^2/m^2)	±10%
Meteorological forcing variables		
SWdown	Downward shortwave radiation (W/m^2)	±10%
LWdown	Downward longwave radiation (W/m^2)	±10%
Tair	Near surface air temperature (K)	±10%
Qair	Near surface specific humidity (kg/kg)	±10%
Rainf	Rainfall rate (mm/s)	±10%
Wind	Surface wind speed (m/s)	±10%
Model state variables		
SoilMoist	Average layer soil moisture (m^3/m^3)	Updated
SoilTemp	Average layer soil temperature (K)	Updated
CanopInt	Canopy intercepted water storage (kg/m^2)	Updated

of each land cover and soil category within each 12-km grid. That is, the area-based soil and land cover data are spatially weighted for each 12-km modeling grid, whereas the grid-based 1-km LAI data set was spatially averaged for each underlying 12-km modeling grid. The forcing data together with the LAI, land cover and soil data were incorporated into the JULES and CABLE models independently, to simulate the temporal evolution of soil moisture. The model grid in both JULES and CABLE was 12-km, with each run at an hourly time step.

The soil moisture observation data used to drive the CABLE and JULES assimilation was the SMOS Level 2 soil moisture, which is reported at the 15-km Discrete Global Grid (DGG). The specific SMOS Level 2 data set used was the Soil Moisture Level 2 v.4.0 User Data Product (SMUDP2), obtained for the period from January to December 2010. It is notable that the SMOS Level 2 v.4.0 soil moisture was retrieved using the Mironov model [39]. In the CABLE and JULES assimilation runs, the SMOS data set was used at the 15-km DGG in accordance with findings from [20], which showed that the error involved in representing the 42-km SMOS observations at the 15-km DGG is not expected to be worse than the noise that currently exists in the original SMOS data [21].

Moreover, the SMOS Level 2 soil moisture was re-scaled to the simulated soil moisture independently for CABLE and JULES, to remove the bias between the observation and model output in line with other studies including [10,11,41,48]. The re-scaling procedure matched the mean and standard deviation of the SMOS soil moisture to the simulated surface soil moisture from the model, according to Eq. (1).

$$\theta^{r}_{obs} = \theta^{ave}_{sim} + \left[\frac{\sigma_{sim}}{\sigma_{obs}}\right] * \left[\theta_{obs} - \theta^{ave}_{obs}\right] \quad (1)$$

where θ^{r}_{obs} is the re-scaled SMOS soil moisture, θ_{obs} is the original SMOS soil moisture, and θ^{ave}_{obs} and σ_{obs} represent the average and standard deviation of the SMOS soil moisture respectively. The θ^{ave}_{sim} and σ_{sim} indicate the average and standard deviation respectively for the simulated soil moisture from the model.

2.2. The evolutionary data assimilation

The EDA procedure applied in this study to assimilate soil moisture into the JULES and CABLE models follows the modeling strategy in [21]. The EDA shown in Fig. 2, is an applied evolutionary strategy which evolves a population of competing members under one or more evaluation objectives through several cycles of evolution. A candidate member in the population is defined by two properties: (i) genotype, representing the internal properties of a member; and (ii) phenotype, being the expressed behavior of a member. The genotype is equivalent to a vector string of values connecting model parameters, initial states, and input forcing data, which make up the internal dynamics of a land surface model, whereas the simulated output (e.g., soil moisture) from the model represents the phenotype. The candidate members in the population undergo competition and natural selection based on the evaluation objectives in phenotype space, while the members evolve in genotype space through variation and reproduction of new members. The variation of members is achieved through mutation operation, which perturbs the genotype string of individual members. The reproduction of members (or crossover operation) combines high performing members to generate new members with the potential to retain quality elements of their genotype string.

The EDA procedure is based on the Non-dominated Sorting Genetic Algorithm – II (NSGA-II), developed by [9]. In the EDA procedure, the initial evolutionary cycle involves the creation of a random population of members, the assessment of the members based on evaluation objectives, and the selection of half of the population members for reproduction. For subsequent cycles of evolution, the selected high performing members are combined with the new members to form a new population which undergoes another evaluation, selection, and reproduction. Each cycle of the evolution of the population members is called a generation. The initial genotype for population members is generated using the minimum and maximum bounds for model parameters, states, and forcing variables as shown in Table 1 for JULES, and Table 2 for CABLE. This initial population is generated using the Latin hypercube sampling, which provides values over the entire length of the variable distributions. Subsequent populations were generated based on the evolutionary operators including tournament selection, mutation and crossover. The evaluation of members in phenotype space is based on the absolute difference in Eq. (2), and the cost function in Eq. (3).

$$AbsDiff = |y_i - y_{o,i}| \quad (2)$$

where y_i is the simulated soil moisture from a population member, $y_{o,i}$ is the observed soil moisture from an observation ensemble member.

$$J = \sum_{i=1}^{t} J(y_i) = \sum_{i=1}^{t} \left\{ \frac{(y_i - y_{b,i})^2}{\sigma_b^2} + \frac{(y_i - y_{o,i})^2}{\sigma_o^2} \right\} \quad (3)$$

where $y_{b,i}$ is the background (i.e., forecast) soil moisture for the ith data point, σ_b^2 is the variance for the background soil moisture, σ_o^2 is the variance for the observation soil moisture, y_i represents the analysis (i.e., the searched) soil moisture for ith data point which minimizes $J(\hat{y}_i)$, and t is the number of data points or the time (note that $t = 1$ in this case for sequential assimilation).

At the referenced (or the last) generation, the final evolved members are chosen as the updated members for the current assimilation time step. The updated members are used to determine the forward estimation, and seeded as the initial population for the next assimilation time step. The above procedure is

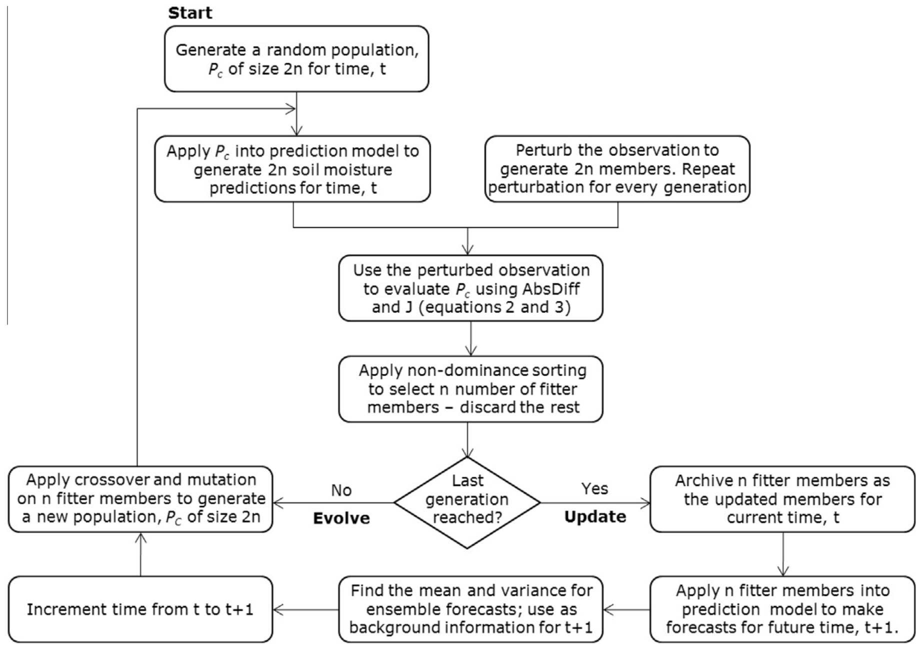

Fig. 2. Computational procedure of the EDA approach, showing the evaluation, selection and reproduction of the population and its update through time (adapted from [17]).

repeated for each assimilation time step to: (i) evolve a population of competing members through several generations, (ii) select and archive the final evolved members as updated members, (iii) use the updated members to determine background (or forward) estimates for future time steps, and (iv) seed the updated members as initial population members for subsequent time periods. Hence, several competing members are evaluated to determine the updated members for each assimilation time step.

2.3. Assessment of uncertainty for model components

The updated ensemble members obtained for each assimilation time step using the EDA approach have unique properties, with the capability to assess model uncertainty due to landscape spatial variability (embedded in model parameters and states), and input forcing data. These sources of uncertainty are embedded in the genotype of updated members. To explore the genotype, it is important to emphasize the unique properties of the updated members obtained from the EDA approach. The updated members are equally accurate (i.e., incomparable based on the evaluation measures) in a way that each member provides a unique compromise between the simulated output and the observation data in phenotype space. Accordingly, the associated genotype accounts for the landscape spatial heterogeneity, through the ensemble model parameters, state variables and meteorological forcing needed to obtain the optimal compromise in phenotype space. As a result, the monitoring of the genotype of updated members through time provides an estimate of the expected landscape spatial variability from the model standpoint, needed to obtain a consistently optimal compromise in phenotype space. The estimation of the landscape spatial variation also follows the procedure outlined in [21].

Given that the updated genotype is a function of the optimal compromise between the simulated output and the observation, an examination of the changes in model parameters, initial states, and input forcing data and their interactions are important to estimate their shared uncertainty. The multi-dimensional monitoring of these three model components (parameters, initial states, and input forcing) across the assimilation time steps provides an estimate of the expected uncertainty for the individual model components. The monitoring in genotype space is conducted using clustering analysis, with one-dimensional clustering applied to determine the minimum landscape spatial variation, and multi-dimensional clustering employed to determine the individual uncertainties for model parameters, states, and input forcing data.

2.4. Setup of model and data assimilation runs

The EDA procedure is applied to assimilate the SMOS soil moisture separately into the JULES and CABLE models at a daily time step from January to December, 2010. A population of 40 members were evolved across 5 generations, with 20 updated members selected for each assimilation time step. That is, for each assimilation time step an ensemble of 200 (i.e. 40×5) members was evaluated, after which 20 optimal ones were selected as the updated members. The initial population members were generated based on the uncertainty intervals for model parameters, states, and input forcing variables in Table 1 for the JULES model, and Table 2 for the CABLE model using the Latin hypercube sampling. For subsequent population members and assimilation time steps, the uncertainty values for model parameters, states, and forcing variables were derived from the population members, with the uncertainties constrained to the lower and upper bounds found in Table 1 for the JULES model, and Table 2 for the CABLE model. It is noted that the original values for model parameters and states were determined by soil and land cover data in concert with the JULES and CABLE models. Based on these original values, the model parameters were perturbed using a relative measure, such that an ensemble value for a model parameter was always relative to the original model parameter value determined from the landscape properties data. Similarly, the input forcing variables were perturbed using a relative measure; the state variables were also perturbed using a relative measure from their updated values.

Given the spatial mismatch between the SMOS 15-km DGG and the 12-km model grid, the 15-km SMOS soil moisture was converted to the 12-km model grid by using the overlapping areas between the 15-km DGG and the respective 12-km model grid as weighting factors. According to [20], soil moisture retrieval and data assimilation applications can use the 15-km SMOS data at the 12-km model grid without downscaling because the estimated errors between the two spatial resolutions are smaller than the standard error of the current SMOS data. The observation uncertainty was based on the soil moisture error which comes along with the SMOS Level 2 soil moisture, with this error being only the model inversion error and not the sensor error. The simulated soil moisture uncertainty was derived adaptively from the updated population members. The simulated soil moisture for the surface layer (i.e., top 3-cm in JULES, and top 2.2-cm in CABLE) were used in the evaluation against the observed SMOS soil moisture, since the SMOS observation is equivalent to the top ~2-cm soil moisture. Following the standard NSGA-II implementation, the EDA uses a crossover probability of 0.8 and a mutation probability of 1/m (where m is the number of variables) to perturb and reproduce new members.

Additionally, a calibration procedure was undertaken to evaluate the updated estimates from both models. The CABLE and JULES models were calibrated to the SMOS soil moisture over the same assimilation time period. The NSGA-II was used to calibrate both models, with 40 members evolved over 250 generations. It is noted that the calibration runs are independent from the data assimilation runs, such that the model calibration results were not used in the assimilation runs. The rationale for the calibration is to provide a robust evaluation of the updated output, instead of using randomly chosen values for model parameters, initial states to generate the open loop estimate.

To assess the soil moisture estimates, three evaluation measures: root mean square error (RMSE) in Eq. (4), bias in Eq. (5), and the normalized error reduction (NER) [5] according to Eq. (6) were used.

$$RMSE = \sqrt{\frac{\sum_{i=1}^{k}(y_i - y_{o,i})^2}{k}} \quad (4)$$

where: $y_{o,i}$ is the observed soil moisture for ith time step, y_i is the simulated soil moisture for ith time step, k is the duration of time period.

$$Bias = \frac{\sum_{i=1}^{k}(y_i - y_{o,i})}{k} \quad (5)$$

$$NER = 1 - \frac{RMSE_u}{RMSE_o} \quad (6)$$

where: $RMSE_o$ and $RMSE_u$ are the RMSE for the open loop and the updated outputs respectively. The NER varies between negative infinity and 1.0, with a negative NER indicating a deterioration of the updated output in comparison to the open loop. A value of NER closer to 1.0 means that the updated output has a greater improvement over the open loop [5].

3. Results and discussion

3.1. Evaluation of the updated soil moisture estimates against SMOS

To assess the soil moisture estimation from CABLE and JULES, we begin with a comparison of open loop estimates at the near-surface soil layer from both models against the SMOS soil moisture.

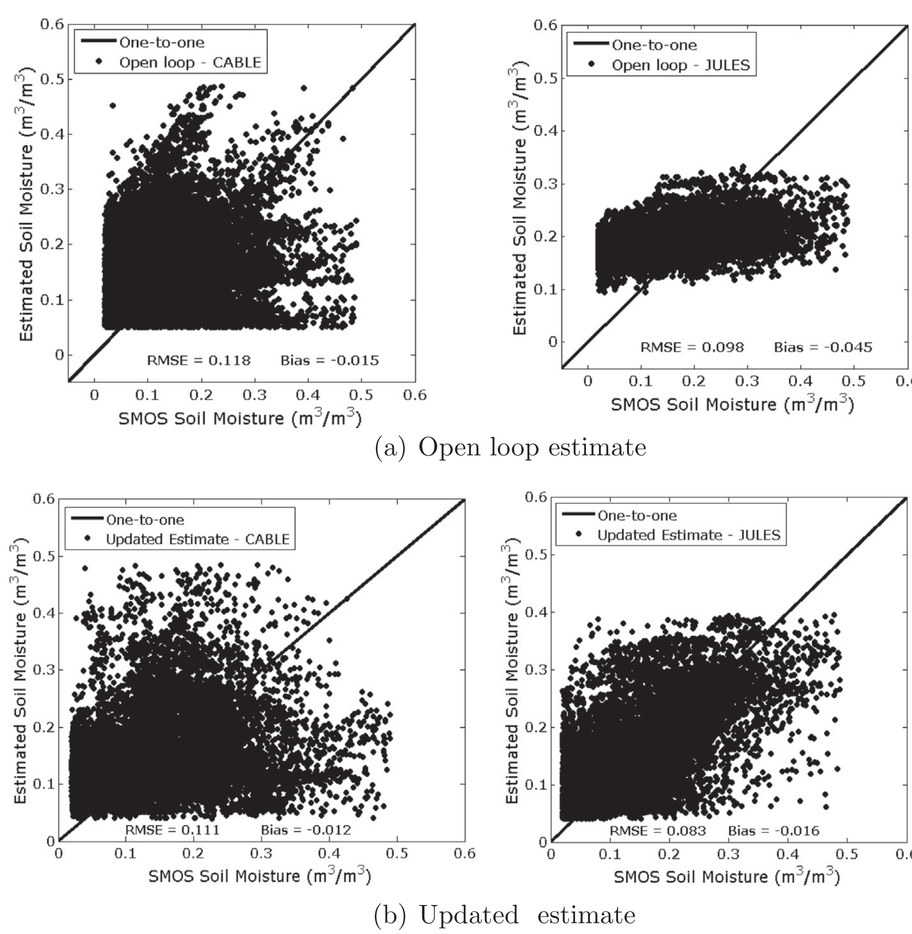

Fig. 3. Evaluation of the open loop (top row) and the updated (bottom row) soil moisture estimates from CABLE (left panel) and JULES (right panel) against the SMOS soil moisture for all model grids.

The comparison of the open loop near-surface estimates for all model grids against the SMOS soil moisture, using two evaluation measures: RMSE and bias is presented in Fig. 3(a). It is noted that the open loop estimate from each model represent their corresponding model calibrated estimates. The JULES estimate is biased for extreme wet and dry moisture conditions, but its RMSE is superior to the CABLE output. The small bias from the CABLE open loop is compromised by large deviations in its near-surface soil moisture from the SMOS data. Given that the JULES output has a smaller RMSE, and that its bias is reasonably close to the soil moisture error (about 0.03 m^3/m^3) from in-situ measurements, the JULES open loop is preferred to the CABLE output. Hereafter the JULES open loop is used in the remainder of the analysis, and is implicitly referred to when discussing the open loop unless the CABLE open loop is specifically referred to.

Table 3
Summary evaluation measure values for CABLE and JULES soil moisture outputs evaluated against SMOS (for all model grids), and in-situ OzNet soil moisture (for all 13 monitoring stations) at the near-surface and deeper soil layers.

Evaluation	Output	RMSE (m^3/m^3)	Bias (m^3/m^3)	NER
SMOS	Open loop – CABLE	0.118	−0.015	
	Open loop – JULES	0.098	−0.045	
	Updated – CABLE	0.111	−0.012	0.059
	Updated – JULES	0.083	−0.016	0.153
OzNet – 8 cm	Open loop – CABLE	0.122	0.042	
	Open loop – JULES	0.121	0.043	
	SMOS	0.111	0.049	
	Updated – CABLE	0.102	−0.005	0.164
	Updated – JULES	0.100	−0.005	0.174
OzNet – 30 cm	Open loop – CABLE	0.121	0.075	
	Open loop – JULES	0.107	0.052	
	Updated – CABLE	0.109	0.001	0.099
	Updated – JULES	0.102	−0.000	0.047

Additionally, the updated soil moisture estimates from CABLE and JULES are compared against the SMOS soil moisture for all model grids in Fig. 3(b). The three evaluation measures are summarized in Table 3. The updated estimates from CABLE and JULES have each improved upon their respective open loop estimates. Based on the evaluation measures, the JULES updated estimate has a slightly more accurate estimate of the SMOS soil moisture than both open loop outputs and the CABLE updated estimate. The bias estimate for the CABLE updated output is the smallest (i.e., most accurate) but its RMSE value is higher (i.e., less accurate) and is comparable to that obtained from the JULES open loop.

Further, spatial plots of the RMSE and bias values at the 12-km model grid for the open loop and the updated estimates from CABLE and JULES are shown in Fig. 4. Across all model grids, the CABLE output is least biased in comparison to the JULES output, whereas the RMSE values from JULES are superior to those obtained from CABLE. It is noted that the updated CABLE output has the least accurate values of RMSE in the spatial plot, but they are better than its open loop estimate as demonstrated in Fig. 3.

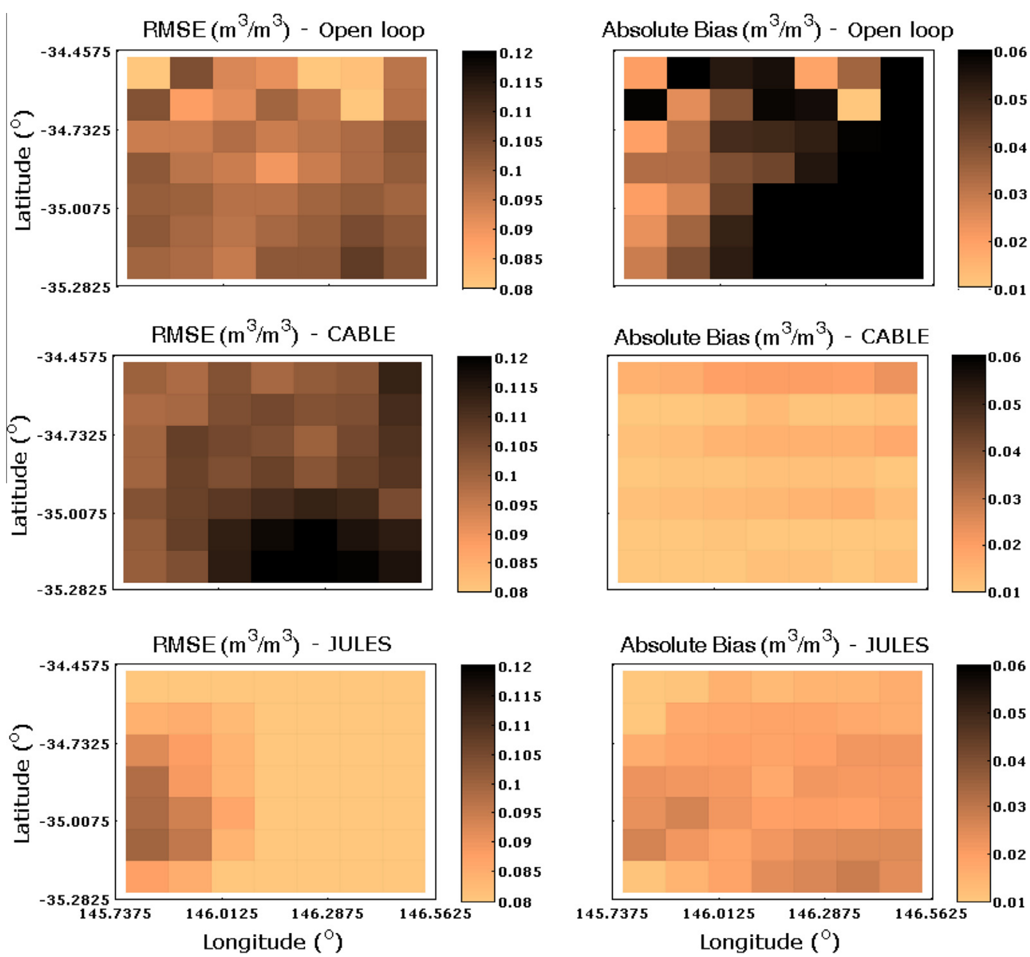

Fig. 4. Spatial plot of the evaluation measures: RMSE and bias for the 12-km model grid based on the evaluation of the open loop (from JULES) and the updated near-surface soil moisture estimates from CABLE and JULES against the SMOS soil moisture.

Finally, a time series comparison of the open loop and updated estimates from CABLE and JULES against the SMOS soil moisture is presented in Fig. 5 for model grids overlapping OzNet monitoring stations Y6 and Y10. There is no preference for the two chosen stations but as will be demonstrated, these same stations are also used at the OzNet evaluation stage. At the Y6 and Y10 model grids, the CABLE open loop shows very little dynamic to capture the wet and dry soil moisture conditions. The JULES open loop has a soil moisture dynamic that is similar to the observed SMOS data but with a mismatched temporal agreement. The updated estimates from CABLE and JULES have improved upon both open loop outputs in terms of dynamics and temporal agreement. The updated CABLE and JULES outputs capture both the peak and troughs of the SMOS soil moisture dynamic. While the updated CABLE estimate has some instances of temporal mismatch, the updated JULES output is wetter (over-estimate) at some extreme wet (peak) conditions, and drier (under-estimate) at some extreme dry (trough) conditions. Overall, the updated JULES output is clearly superior to the CABLE output, capturing the peaks and troughs at the right time periods.

3.2. Evaluation of the updated soil moisture estimates against in-situ OzNet

To begin the evaluation against the in-situ OzNet data, the open loop outputs from CABLE and JULES are first compared against the OzNet soil moisture for all 13 monitoring stations for the near-surface soil layer (0–8 cm) in Fig. 6. The results show that both open loop outputs have almost the same RMSE and bias values, indicating similar performance. Second, the updated estimates from

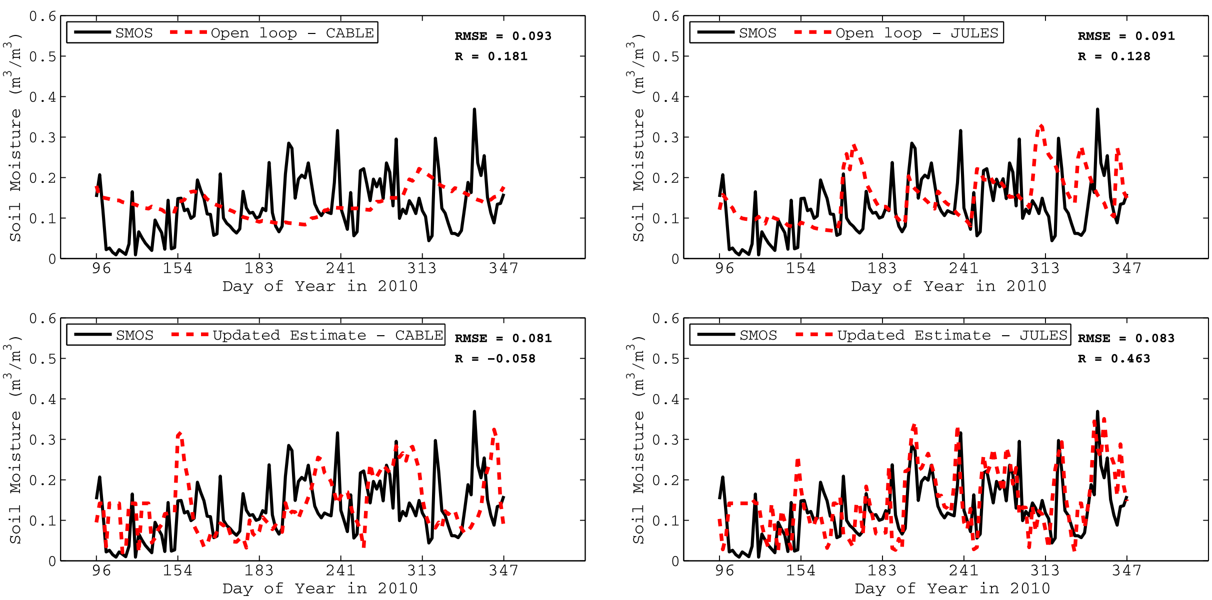

(a) model grid overlapping Y6

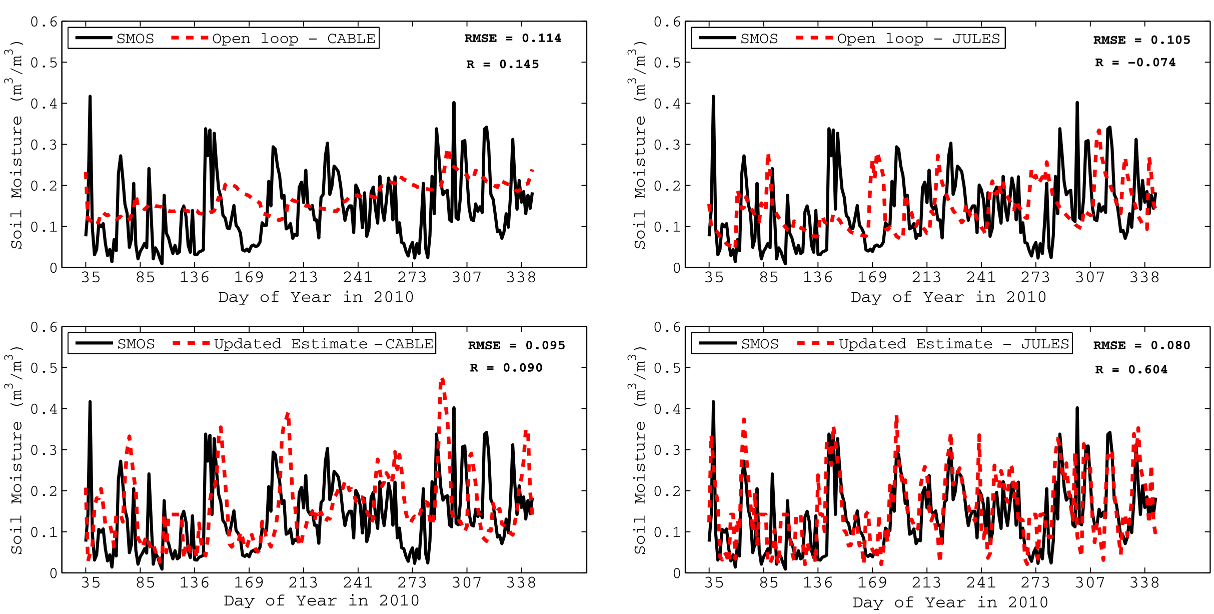

(b) model grid overlapping Y10

Fig. 5. Time series comparison of open loop and updated near-surface soil moisture from CABLE (left panel) and JULES (right panel) against SMOS soil moisture at stations Y6 and Y10.

CABLE and JULES along with the SMOS soil moisture are evaluated against the near-surface (0–8 cm) in-situ OzNet soil moisture in Fig. 7. The rationale to include the SMOS data in this comparison is to illustrate that there are significant differences between these two data sets: the SMOS and in-situ point-based data. The updated CABLE and JULES outputs and the SMOS data have improved upon the evaluation measures obtained from both open loop estimates. The overall comparison based on RMSE and bias shows that the updated estimate from JULES provides the most accurate estimate of the in-situ observation, with the SMOS being the least accurate. It is noted that the updated estimates from both CABLE and JULES have almost the same accuracy based on the RMSE and bias values.

Third, the updated root-zone estimates from CABLE and JULES and the open loop (from JULES) are evaluated against the deeper (0–30 cm) in-situ OzNet soil moisture in Fig. 8. The estimated evaluation measures for both the surface and deeper soil layers are summarized in Table 3. While the soil moisture updates in CABLE had the largest RMSE, the updated estimates from CABLE and JULES

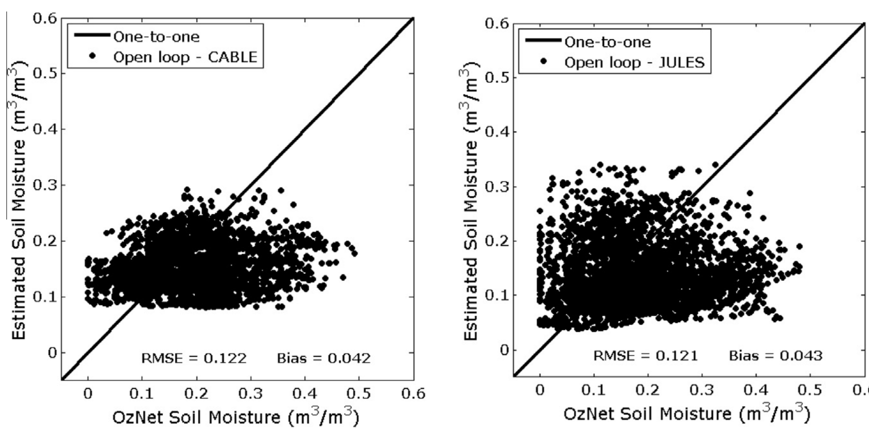

Fig. 6. Evaluation of the open loop soil moisture estimates from CABLE (left panel) and JULES (right panel) against the OzNet soil moisture at the near-surface soil layer for all 13 monitoring stations.

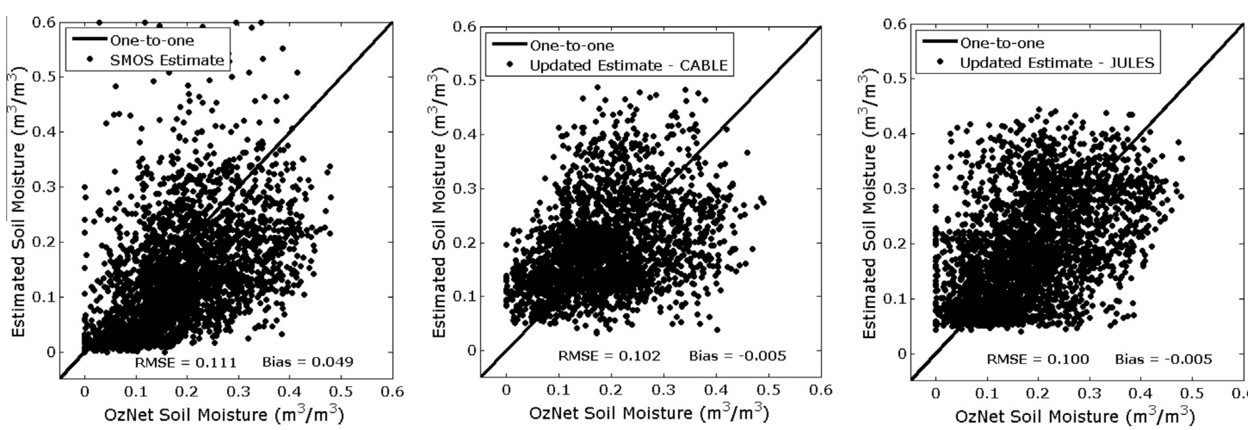

Fig. 7. Evaluation of the SMOS, open loop, and the updated CABLE and JULES estimates of near-surface soil moisture against the 0–8 cm in-situ OzNet soil moisture for all 13 monitoring stations.

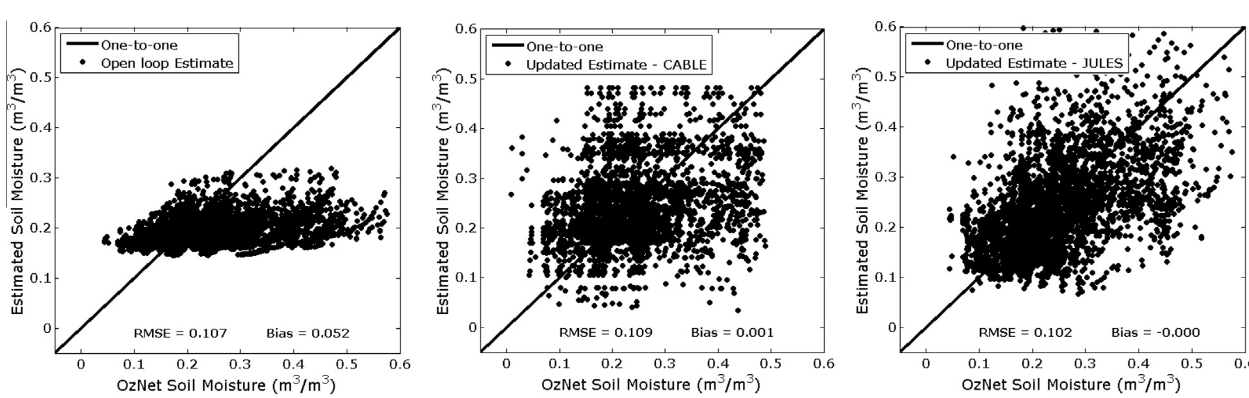

Fig. 8. Evaluation of the open loop (from JULES), and the updated CABLE and JULES estimates against the deeper (0–30 cm) in-situ OzNet soil moisture for all 13 monitoring stations.

both had a lower (i.e., more accurate) bias values than the open loop (JULES) when compared to in-situ data, with JULES having a slightly superior estimate of soil moisture than those obtained from CABLE.

A time series comparison of the open loop and updated estimates from CABLE and JULES against the in-situ OzNet soil moisture for the near-surface layer is presented in Fig. 9 for model grids overlapping OzNet monitoring stations Y6 and Y10. The CABLE output for both open loop and updated estimate show very little dynamic with respect to the OzNet soil moisture, whereas the JULES outputs are highly dynamic, but with some instances of a temporal mismatch. The updated estimates from CABLE and JULES have improved upon both open loop outputs in terms of RMSE evaluation. The updated JULES output provides a superior estimate of the OzNet data in terms of soil moisture dynamics, temporal agreement and RMSE evaluation. It is noted that the updated JULES output is wetter at some peaks and drier at some troughs, but its overall soil moisture dynamics is more in agreement with the in-situ OzNet than the CABLE outputs.

Finally, the seasonality of soil moisture estimation is examined for the updated CABLE and JULES outputs using the in-situ OzNet data for both the surface and deeper soil layers. The OzNet and the updated soil moisture are divided into four seasons, namely Season 1 comprising December, January, and February (DJF), Season 2 comprising March, April, and May (MAM), Season 3 comprising June, July, and August (JJA), and September, October, and

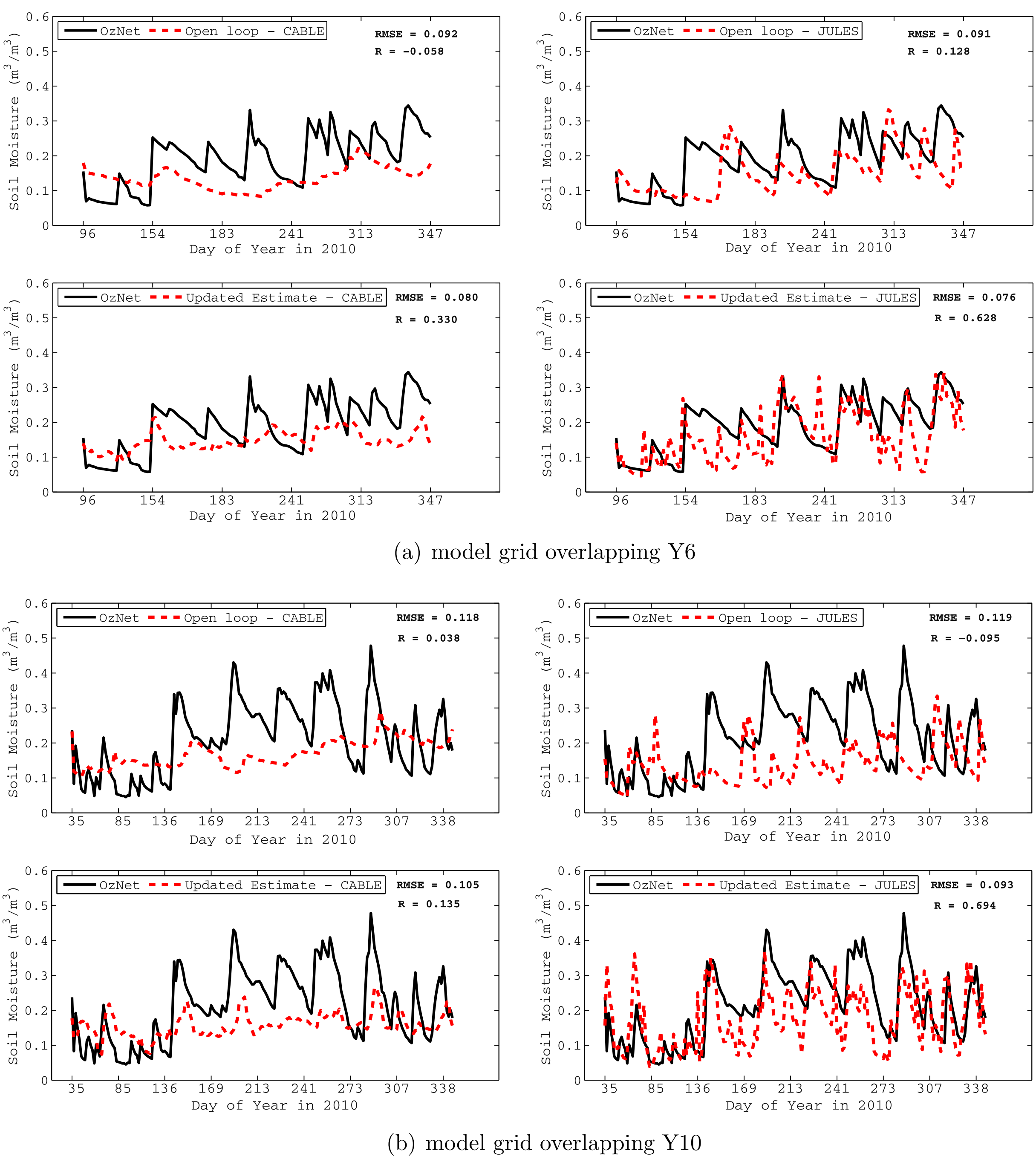

Fig. 9. Time series comparison of open loop and updated estimates of near-surface soil moisture from CABLE (left panel) and JULES (right panel) against the 0–8 cm in-situ OzNet soil moisture at stations Y6 and Y10.

November (SON) making up Season 4. The RMSE and bias values are determined using data from each season. The evaluation of the updated CABLE and JULES outputs against the in-situ OzNet soil moisture for all 13 monitoring stations for both surface and deeper soil layers in each season is presented in Table 4. Soil moisture is most accurately estimated in the MAM season, with the wet JJA season having the least accuracy. Overall, accurate estimation of soil moisture favor the dry (DJF) and dry-to-wet (MAM) seasons than the wet (JJA) and wet-to-dry (SON) seasons. Both CABLE and JULES outputs have similar RMSE and bias values across the 4 seasons for both near-surface and deeper soil depths.

Overall, the assessment of the updated soil moisture in all the experiments show that the JULES output has consistently performed slightly better than the CABLE estimate based on the evaluation measures. While the accuracy difference is negligible between CABLE and JULES based on the OzNet near-surface soil moisture, the JULES model provided a significantly improved soil moisture estimate at the deeper soil layer.

3.3. Assessment of model component uncertainties

The intercomparison between the updated soil moisture estimates from CABLE and JULES is important. But equally important is the assessment of how the models respond to changes in decision space. For land surface models, the changes in decision space encompass crucial uncertainties for model components which have direct impact on the simulated output from the models. As a result, the updated ensemble members from both CABLE and JULES were analyzed to determine the commonality of model parameter values which remain persistent across assimilation time periods. The assessment of the updated members was undertaken using clustering analysis, which is suited to determining persistent values of model parameters/variables across several assimilation time steps. The clustering analysis was performed for each model parameter/variable, and the frequency based dominant cluster determined as the persistent interval within which the model mostly finds the updated estimate for each assimilation time period. It is noted that for each model parameter/variable, a test of clustering has been performed according to the knee method [45]. The knee method has also been used to determine the appropriate number of groups needed to cluster each variable. Overall, the number of clusters ranged from 5 to 9.

Table 4
Seasonal variations of soil moisture estimation based on the evaluation of updated estimates from CABLE and JULES against in-situ OzNet soil moisture across all 13 monitoring stations for the near-surface and deeper soil layers.

Season	Model	RMSE (m^3/m^3)		Bias (m^3/m^3)	
		0–8 cm	0–30 cm	0–8 cm	0–30 cm
DJF	CABLE	0.093	0.082	−0.006	0.016
	JULES	0.104	0.095	−0.019	0.008
MAM	CABLE	0.082	0.095	−0.009	0.043
	JULES	0.076	0.086	−0.020	0.009
JJA	CABLE	0.095	0.143	0.057	0.104
	JULES	0.091	0.138	0.046	0.097
SON	CABLE	0.100	0.130	0.048	0.094
	JULES	0.103	0.127	0.038	0.087

The original intervals of the model parameters/variables, together with the updated bound and the dominant cluster, are shown in Fig. 10 for the CABLE model and in Fig. 11 for the JULES model. The updated bound is represented by the minimum and maximum values of the updated ensemble members obtained across all assimilation time steps. As the intervals for different model parameters/variables vary, they have been re-scaled to a unit scale (0.0–1.0) for presentation purposes. For the CABLE output, the area covered by the updated bound as a fraction of the original interval is about 82%, representing a 12% reduction of the original bound. The dominant cluster has covered about 35% of the original bound, representing a 65% reduction of the original interval. The clustering analysis performed on the updated members has reduced the coverage of its searched area by 57%, as the area covered by the dominant clusters with respect to the updated bound is 43%.

For the updated JULES output, the area covered by the updated bound as a fraction of the original interval is 68%, representing a 32% reduction of the original bound. The dominant cluster has covered 45% of the original bound, which amounts to a 55% reduction of the original interval. The clustering analysis performed on the updated members has reduced the coverage of its searched area by 34%, as the area covered by the dominant clusters with respect to the updated bound is 66%.

These findings point to crucial differences in the internal dynamics of both models. The update bound in the CABLE output is large in comparison to the JULES output, but the assessment of the updated members showed that there is a high level of instability in the CABLE output. The high reduction of the updated bound by the dominant cluster in the CABLE output means that the temporally persistent members are sensitive. This is because the updated members which were found to be persistent across assimilation

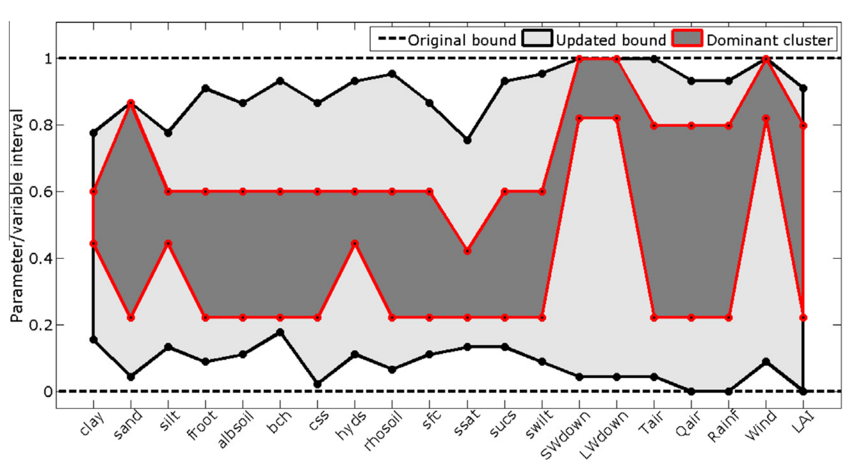

Fig. 10. Comparison of the scaled intervals of CABLE model parameters/variables for the original bound, the updated bound obtained from the EDA procedure, and the dominant cluster obtained through clustering analysis of the updated members.

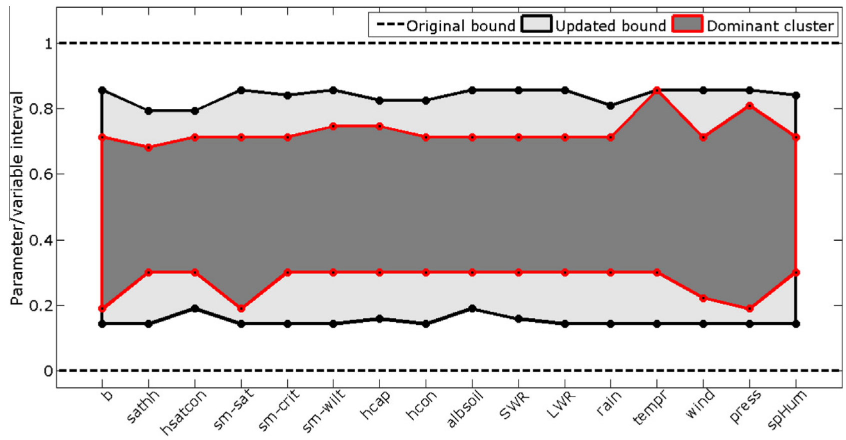

Fig. 11. Comparison of the scaled intervals of JULES model parameters/variables for the original bound, the updated bound obtained from the EDA procedure, and the dominant cluster obtained through clustering analysis of the updated members.

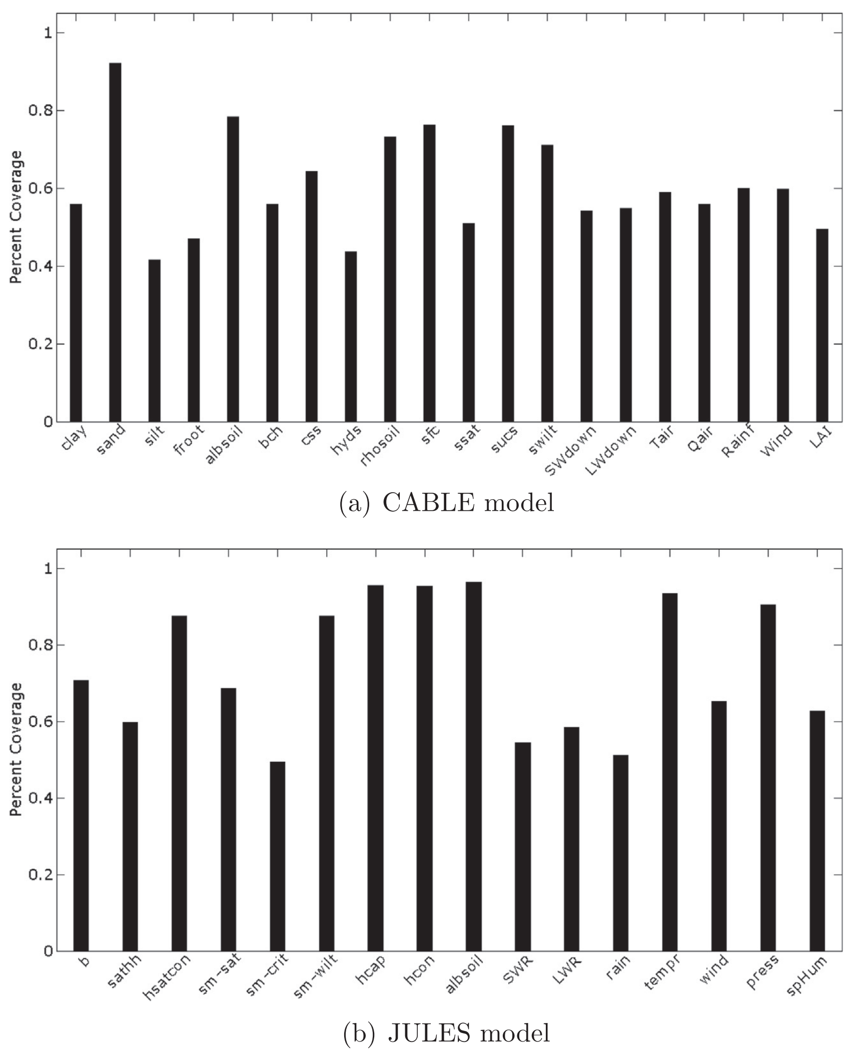

Fig. 12. Level of convergence indicated by frequency based coverage of the updated bound for model parameters/variables of CABLE and JULES models.

time periods are located in smaller regions of the updated bound, such that small changes around these regions will cause significant changes in the soil moisture model response. It is noted that the high reduction of the updated bound is advantageous for generating a small number of ensemble members leading to a manageable number of prediction scenarios.

The updated JULES output and its associated dominant cluster are relatively stable in comparison to the updated CABLE output. The temporally persistent members in the dominant cluster cover a large (i.e., 66%) portion of the updated bound, such that small changes around the dominant clusters will not lead to significant changes in the model soil moisture response. While the JULES dominant clusters are not sensitive, a large number of ensemble members are needed to cover the wide range of its model parameters/variables. Additionally, it is important to point out that both models respond differently to the common forcing variables, including precipitation, air temperature, wind speed, and incoming short and long wave radiation, and specific humidity. Notable among these variables for the CABLE dominant clusters is wind speed, incoming short and long wave radiation. The CABLE output requires higher increments consistently on the original values of these three variables, whereas the JULES output has characteristically broad range with instances of both high and low increments.

Additionally, the frequency based coverage of each model parameter/variable in the dominant clusters for the CABLE and JULES outputs are shown in Fig. 12. The frequency based coverage is equivalent to the level of convergence for each model parameter/variable. Overall, the JULES dominant clusters show a relatively higher level of convergence than the CABLE output. The high level of convergence in the JULES output is partly due to a wider range for its dominant clusters, which generally incorporate more updated members. High convergence levels usually signify a less sensitive model parameter/variable, meaning that the dominant cluster found is also located at the most populated region frequency-wise. This is evident in the results presented, with less sensitive and stable dominant clusters in Fig. 11, supported by high convergent model parameters/variables in the JULES output. Conversely, the relatively sensitive dominant clusters in Fig. 10 are associated with a less convergent model parameters/variables in the CABLE output.

4. Summary and conclusion

This study has undertaken an intercomparison between the CABLE and JULES models in terms of daily soil moisture estimation in the Yanco area, southeast Australia. The intercomparison involved an examination of the differences and similarities of soil moisture estimation for both near-surface and deeper soil layers, together with an assessment of the internal dynamics of both models. The SMOS Level 2 soil moisture was assimilated into both models to determine the updated ensemble estimate. An evaluation of the updated estimate showed that, in general, the SMOS assimilation into both models provided an improved estimate of soil moisture when compared to the open loop estimate for both surface and deeper soil layers. Overall, the updated JULES soil moisture output was found to be slightly more accurate than those from the CABLE model at both near-surface and deeper soil layers.

The updated members from both models were also analyzed in decision space using clustering analysis to determine temporally persistent members with the highest level of commonality across assimilation time periods. The updated ensemble membership in decision space is equivalent to the internal dynamics of the model, since it encompasses crucial model components including model parameters, states, and input forcing variables. The assessment of the internal dynamics of the models showed that the updated membership from both models have a similar coverage of the original bound for their respective model parameters and variables. However, their temporally persistent memberships were different, with the CABLE output being relatively more sensitive than that from the JULES output in terms of soil moisture estimation. The dominant clusters from the CABLE output were also found to be less convergent, whereas the JULES output showed higher levels of convergence.

An important finding of this study was that while satellite remote sensing data are usually assimilated into land surface models to improve their prediction skill, these data sets also provide a unique avenue to learn about the model performance under different meteorological conditions. As demonstrated in this study, both CABLE and JULES were found to respond to some parameters/variables in a persistent way by biasing either positively or negatively their original values under changing meteorological conditions. Across the assimilation time periods, CABLE was found to be sensitive in a way that the updated members were found persistently within small fractions of the entire search space, thus providing the opportunity to isolate model response to specific variables. These findings provide a further diagnostic framework for examining model behavior under changing environment conditions, together with unique pathways towards examination of weaknesses in model structure. It is noted that these findings are subject to the Yanco area for soil moisture estimation only, and that additional investigations are needed to uncover more information for each model and for other catchments. The interpretation of these findings is also constrained by the limited modeling time period, mainly due to the scarcity of consistent forcing and observation data sets. However, the key finding is the provision a model diagnostic framework to intercompare land surface models on the basis of their temporal stability in model decision space.

The findings in the study point to additional questions for consideration. While this study has shown that the models respond differently to some input forcing variables, there is the need for further investigation to determine landmarks in decision space which will correspond to specific model response. That is, a methodology is needed to map the decision space in a way that: (i) model structural weaknesses can be quickly identified, (ii) changes in landscape and meteorological fluctuations can be accounted for and mapped onto decision space, and (iii) subsets of the decision space can be attributed to specific model response(s).

Acknowledgments

This research was supported by funding from the Australian Research Council (LP0989441). The authors wish to thank both anonymous reviewers for their comments.

References

[1] Balsamo G, Beljaars A, Scipal K, Viterbo P, van den Hurk B, Hirschi M, et al. A revised hydrology for the ECMWF model: verification from field site to terrestrial water storage and impact in the integrated forecast system. J. Hydrometeorol. 2009;10(3):623–43. http://dx.doi.org/10.1175/2008JHM1068.1.

[2] Best MJ, Pryor M, Clark DB, Rooney GG, Essery RLH, Mnard CB, et al. The joint UK land environment simulator (JULES), model description – Part 1: Energy and water fluxes. Geosci Model Dev Discuss 2011;4:595–640. http://dx.doi.org/10.5194/gmdd-4-595-2011.

[3] Boone A et al. The AMMA land surface model intercomparison project. Bull Am Meteorol Soc 2009;90:187–208. http://dx.doi.org/10.1175/2009BAMS2786.1.

[4] Operational implementation of the access numerical weather prediction systems. NMOC Oper Bull 83:1–34.

[5] Chen F, Crow WT, Starks PJ, Moriasi DN. Improving hydrologic predictions of a catchment model via assimilation of surface soil moisture. Adv Water Resour 2011;34(4):526–36.

[6] Clapp R, Hornberger G. Empirical equations for some soil hydraulic properties. Water Resour Res 1978;14(4):601–4.

[7] Crow WT, Wood EF. The assimilation of remotely sensed soil brightness temperature imagery into a land surface model using ensemble Kalman filtering: a case study based on ESTAR measurements during SGP97. Adv Water Resour 2003;26(2):137–49.

[8] de Rosnay P, Drusch M, Vasiljevic D, Balsamo G, Albergel C, Isaksen L. A simplified extended Kalman filter for the global operational soil moisture analysis at ECMWF. Q J R Meteorol Soc 2013;139(674):1199–213. http://dx.doi.org/10.1002/qj.2023.

[9] Deb K, Pratap A, Agrawal S, Meyarivan T. A fast and elitist multiobjective genetic algorithm: NSGA-II. IEEE Trans Evol Comput 2002;6(2):182–97.

[10] Dee DP, Da Silva AM. Data assimilation in the presence of forecast bias. Q J R Meteorol Soc 1998;124(545):269–95. http://dx.doi.org/10.1002/qj.49712454512.

[11] Dee DP, Gaspari G, Redder C, Rukhovets L, da Silva AM. Maximum-likelihood estimation of forecast and observation error covariance parameters. Part ii: Applications. Am Meteorol Soc Mon Weather Rev 1999;127(8):1835–49.

[12] Dharssi I, Bovis K, Macpherson B. Operational assimilation of ASCAT surface soil wetness at the met office. Hydrol Earth Syst Sci 2011;15:2729–46. http://dx.doi.org/10.5194/hess-15-2729-2011.

[13] Dirmeyer PA, Dolman AJ, Sato N. The global soil wetness project: a pilot project for global land surface modeling and validation. Bull Am Meteorol Soc 1999;80(5):851–78.
[14] Dirmeyer PA, Gao X, Oki T. GSWP-2: the second global soil wetness project science and implementation plan. International GEWEX Project Office Publication Series 37;2002:65p.
[15] Dirmeyer PA, Gao X, Zhao M, Guo Z, Oki T, Hanasaki N. The second global soil wetness project (GSWP-2): multi-model analysis and implications for our perception of the land surface. COLA technical report; 2005. 45p.
[16] Draper CS, Walker JP, Steinle PJ, De Jeu RAM, Holmes TRH. Evaluation of AMSR-E derived soil moisture over Australia. Remote Sens Environ 2009;113:703–10. http://dx.doi.org/10.1016/j.rse.2008.11.011.
[17] Dumedah G. Formulation of the evolutionary-based data assimilation, and its practical implementation. Water Resour Manage 2012;26(13):1–18. http://dx.doi.org/10.1007/s11269-012-0107-0.
[18] Dumedah G, Berg AA, Wineberg M. An integrated framework for a joint assimilation of brightness temperature and soil moisture using the non-dominated sorting genetic algorithm-II. J Hydrometeorol 2011;12(2):1596–609. http://dx.doi.org/10.1175/JHM-D-10-05029.1.
[19] Dumedah G, Coulibaly P. Evaluating forecasting performance for data assimilation methods: the ensemble Kalman filter, the particle filter, and the evolutionary-based assimilation. Adv Water Resour 2013;60:47–63. http://dx.doi.org/10.1016/j.advwatres.2013.07.007.
[20] Dumedah G, Walker JP, Rüdiger C. Can SMOS data be used directly on the 15 km discrete global grid? IEEE Trans Geosci Remote Sens 2013;99:1–7. http://dx.doi.org/10.1109/TGRS.2013.2262501.
[21] Dumedah G, Walker PJ. Evaluation of model parameter convergence when using data assimilation in soil moisture estimation. J Hydrometeorol 2014;15:359–75. http://dx.doi.org/10.1175/JHM-D-12-0175.1.
[22] Ferguson CR, Wood EF, Vinukollu RK. A global intercomparison of modeled and observed land–atmosphere coupling. J Hydrometeorol 2012;13:749784. http://dx.doi.org/10.1175/JHM-D-11-0119.1.
[23] Gupta HV, Clark MP, Vrugt JA, Abramowitz G, Ye M. Towards a comprehensive assessment of model structural adequacy. Water Resour Res 2012;48(W08301):1–16. http://dx.doi.org/10.1029/2011WR011044.
[24] Gupta HV, Wagener T, Liu Y. Reconciling theory with observations: elements of a diagnostic approach to model evaluation. Hydrol Process 2008;22(18):3802–13. http://dx.doi.org/10.1002/hyp.6989.
[25] Henderson-Sellers A, Brown VB. Project for intercomparison of landsurface parameterization schemes (PILPS): first science plan. GEWEX technical note. IGPO Publication Series No. 5; 1992. 53p.
[26] Henderson-Sellers A, Pitman AJ, Love PK, Irannejad P, Chen TH. The project for intercomparison of land surface parameterization schemes (PILPS): phases 2 and 3. Bull Am Meteorol Soc 1995;76(4):489–503.
[27] Henderson-Sellers A, Yang Z-L, Dickinson R. The project of intercomparison of land-surface parameterization schemes. Bull Am Meteorol Soc 1993;74(7):1335–49.
[28] Jimènez C et al. Global intercomparison of 12 land surface heat flux estimates. J Geophys Res 2011;116(D02102). http://dx.doi.org/10.1029/2010JD014545.
[29] Jones D, Wang W, Fawcett R, Grant I. Climate data for the Australian water availability project. Australian water availability project milestone report, Bur. Met. Australia; 2007. 37p.
[30] Jones DA, Wang W, Fawcett R. High-quality spatial climate data-sets for Australia. Aust Meteorol Oceanogr J 2009;58:233–48.
[31] Kowalczyk EA, Wang YP, Law RM, Davies HL, McGregor JL, Abramowitz G. The CSIRO atmosphere biosphere land exchange (CABLE) model for use in climate models and as an offline model. CSIRO marine and atmospheric research paper 013, Aspendale, Vic; 2006.
[32] Liang X, Guo J. Intercomparison of land-surface parameterization schemes: sensitivity of surface energy and water fluxes to model parameters. J Hydrol 2003;279(1–4):182–209.
[33] Lymburner L, Tan P, Mueller N, Thackway R, Lewis A, Thankappan M, Randall L, Islam A, Senarath U. The national dynamic land cover dataset (DLCD), record 2011/31, www.ga.gov.au/landcover. Tech. rep., Geoscience Australia; 2011.
[34] Mahanama SPP, Koster RD. Intercomparison of soil moisture memory in two land surface models. J Hydrometeorol 2003;4:1134–46. http://dx.doi.org/10.1175/1525-7541.
[35] Mahfouf J-F. Assimilation of satellite-derived soil moisture from ASCAT in a limited-area NWP model. Q J R Meteorol Soc 2010;136(648):784–98. http://dx.doi.org/10.1002/qj.602.
[36] Margulis AS, McLaughlin D, Entekhabi D, Dunne S. Land data assimilation and estimation of soil moisture using measurements from the southern great plains 1997 field experiment. Water Resour Res 2002;38(12):1299. http://dx.doi.org/10.1029/2001WR001114.
[37] McKenzie N, Jacquier D, Ashton L, Cresswell H. Estimation of soil properties using the atlas of Australian soils. Tech. rep., CSIRO land and water technical report 11/00. Available from <ttp://www.clw.csiro.au/publications/technical2000/>; 2000.
[38] McKenzie NJ, Hook J. Interpretations of the atlas of australian soils. consulting report to the environmental resources information network (erin). Tech. rep., CSIRO division of soils technical report 94; 1992.
[39] Mironov VL, Dobson MC, Kaupp V, Komarov SA, Kleshchenko VN. Generalized refractive mixing dielectric model for moist soils. IEEE Trans Geosci Remote Sens 2004;42(4):773–85.
[40] Pitmana A, Henderson-Sellersb A. Recent progress and results from the project for the intercomparison of land surface parameterization schemes. J Hydrol 1998;212–213:128–35.
[41] Reichle RH, Koster RD. Bias reduction in short records of satellite soil moisture. Geophys Res Lett 2004;31(19):L19501. http://dx.doi.org/10.1029/2004GL020938.
[42] Richards L. Capilliary conduction of liquids through porous mediums. Physics 1931;1:318–33.
[43] Ruti PM et al. The west African climate system: a review of the AMMA model inter-comparison initiatives. Atmos Sci Lett 2011;12(1):116–22. http://dx.doi.org/10.1002/asl.305.
[44] Smith AB, Walker JP, Western AW, Young RI, Ellett KM, Pipunic RC, et al. The Murrumbidgee soil moisture monitoring network data set. Water Resour Res 2012;48(W07701). http://dx.doi.org/10.1029/2012WR011976.
[45] Thorndike RL. Who belong in the family? Psychometrika 1953;18(4).
[46] Walker J, Willgoose G, Kalma J. Three-dimensional soil moisture profile retrieval by assimilation of near-surface measurements: simplified Kalman filter covariance forecasting and field application. Water Resour Res 2002;38(12):1301.
[47] Wang YP, Kowalczyk E, Leuning R, Abramowitz G, Raupach MR, Pak B, et al. Diagnosing errors in a land surface model (CABLE) in the time and frequency domains. J Geophys Res 2011;116:1–18. http://dx.doi.org/10.1029/2010JG001385.
[48] Yilmaz MT, Crow WT. The optimality of potential rescaling approaches in land data assimilation. J Hydrometeorol 2013;14(2):650–60. http://dx.doi.org/10.1175/JHM-D-12-052.1.